Spectrochimica Acta Part B 64 (2009) 1020–1027

Contents lists available at ScienceDirect

Spectrochimica Acta Part B

journal homepage: www.elsevier.com/locate/sab

The effect of sequential dual-gas testing on laser-induced breakdown spectroscopy-based discrimination: Application to brass samples and bacterial strains ☆

Steven J. Rehse *, Qassem I. Mohaidat [1]

Department of Physics and Astronomy, Wayne State University, Detroit, MI 48201, United States

ARTICLE INFO

Article history:
Received 24 November 2008
Accepted 22 July 2009
Available online 3 August 2009

Keywords:
Laser-induced breakdown spectroscopy (LIBS)
Bacteria identification
Brass
Discriminant function analysis (DFA)
Argon
Helium

ABSTRACT

Four Cu–Zn brass alloys with different stoichiometries and compositions have been analyzed by laser-induced breakdown spectroscopy (LIBS) using nanosecond laser pulses. The intensities of 15 emission lines of copper, zinc, lead, carbon, and aluminum (as well as the environmental contaminants sodium and calcium) were normalized and analyzed with a discriminant function analysis (DFA) to rapidly categorize the samples by alloy. The alloys were tested sequentially in two different noble gases (argon and helium) to enhance discrimination between them. When emission intensities from samples tested sequentially in both gases were combined to form a single 30-spectral line "fingerprint" of the alloy, an overall 100% correct identification was achieved. This was a modest improvement over using emission intensities acquired in argon gas alone. A similar study was performed to demonstrate an enhanced discrimination between two strains of *Escherichia coli* (a Gram-negative bacterium) and a Gram-positive bacterium. When emission intensities from bacteria sequentially ablated in two different gas environments were combined, the DFA achieved a 100% categorization accuracy. This result showed the benefit of sequentially testing highly similar samples in two different ambient gases to enhance discrimination between the samples.

1. Introduction

It is well known that time-resolved laser-induced breakdown spectroscopy (LIBS) is a powerful tool for elemental analysis [1]. There are many experimental parameters that can affect the laser-induced plasma, and currently the wide variety of experimental configurations that exist in the numerous labs performing LIBS measurements is a limitation to the standardization of the technique [2,3]. Along with laser wavelength, pulse energy, pulse duration, beam waist and time-resolved gate delay (to name a few), the atmosphere in which the ablation occurs is one of the important experimental parameters that strongly affect the emission characteristics of the plasma [4]. Several studies have been performed in order to investigate the influence of various buffer gases on the plasma formation. Sdorra and Niemax studied the effect of different ambient gases (argon, neon, helium, nitrogen, and air) in the production of plasma by using a nanosecond Nd:YAG laser on a copper sample [5]. The results showed that argon produced a higher plasma temperature and a higher electron density compared with densities obtained from other gases under fixed experimental conditions. Kuzuya et al. investigated the affects of laser energy and surrounding atmosphere on the emission characteristics of the produced plasma [6]. The results showed that the maximum spectral intensity was obtained in argon when the pressure was 200 Torr and at a higher laser energy of 95 mJ. Wisbrun et al. found that an argon atmosphere was most favorable in terms of higher analyte emission intensity and better reproducibility [7]. Moreover, Rehse et al. investigated the importance of atmosphere above the surface of laser-ablated pure water samples and concluded that argon produced a higher temperature and electron density in these plasmas (compared to air or dry nitrogen) but the largest effect was on the temporal evolution of the emission from the plasma, particularly from hydrogen atoms and recombining molecular species [8].

Due to the sensitivity of the plasma emission characteristics on the ambient gas environment, the aim of this experiment was to investigate the effect that sequential testing in two ambient gas environments at atmospheric pressure would have on the ability to identify or discriminate between highly similar samples of bacteria and less-similar samples of brass based on their LIBS spectra. In both the brass alloy and the bacterial system, sequential LIBS analysis in argon and helium yielded an enhanced discrimination between highly similar targets when LIBS emission intensities were analyzed with a discriminant function analysis (DFA). This enhanced discrimination ability was

☆ This paper was presented at the 5th International Conference on Laser-Induced Breakdown Spectroscopy (LIBS 2008), held in Berlin, Adlershof, Germany, 22–26 September 2008, and is published in the Special Issue of Spectrochimica Acta Part B, dedicated to that conference.

* Corresponding author. Tel.: +1 313 577 2411; fax: +1 313 577 3932.
E-mail addresses: rehse@wayne.edu (S.J. Rehse), mohaidat_76@yahoo.com (Q.I. Mohaidat).
[1] Fax: +1 313 577 3932.

0584-8547/$ – see front matter © 2009 Elsevier B.V. All rights reserved.
doi:10.1016/j.sab.2009.07.012

evidenced by an increase in the overall accuracy of identification and an increase in the magnitude of the between-group variances.

2. Experimental

Initial experiments were performed on four Cu–Zn brass alloys with different stoichiometries and compositions ablated first in argon, then in helium. The brass samples were chosen as a representative test system to optimize reproducibility due to the simplicity in sample preparation, surface flatness, and high (relative) alloy homogeneity. Subsequently, the experiment was performed on bacterial samples, with which it was significantly more difficult to produce reproducible measurements.

2.1. LIBS instrumentation

In our experiment we used 10 ns laser pulses from an Nd:YAG laser (Spectra Physics LAB-150–10) as is used in many LIBS experiments (Fig. 1). This laser operates at its fundamental wavelength of 1064 nm. A spatial mode cleaner consisting of a 3× telescopic beam expander was used to expand the beam from its nominal beam diameter of 9 mm to 27 mm prior to the final focusing lens. An iris with a 9 mm diameter following the expanded beam reduced the beam back to its initial diameter. A helium–neon laser at 632.8 nm was overlayed with the infra-red laser beam by using a beam splitter (50:50 @ 633 nm) for visualization. The two laser beams passed through another beam splitter which allowed a CCD camera to image the magnified region on the sample. A 5× microscope objective with a 40 mm working distance was used to focus both laser beams on the target. An optical fiber with 600 μm core diameter was used to collect the optical emission from the microplasma. This fiber was connected to an Èchelle spectrometer (LLA Instruments GmbH, ESA 3000) equipped with a 1024×1024 pixel (24 μm×24 μm) ICCD (Intensified Charged Coupled Device) array, which provided spectral coverage from 200 to 840 nm.

All LIBS testing was done in a small purge gas box mounted on an x–y translation stage. This box (5 cm×7 cm×9 cm) was coupled to the microscope objective by a flexible coupling boot, allowing the chamber to translate freely while remaining relatively air tight. Gases were introduced to the chamber through a 6.35 mm flexible plastic tube that penetrated the coupling boot. Gas was inlet at a volumetric flow rate of approximately 8×10^{-5} m^3/s and a slight overpressure was achieved in the intentionally leaky box. Given the small size of the purge box, it took no more than 1 min for a new gas to completely displace the old gas in the box. Samples were introduced through a magnetically sealable door. Thus, it took very little time to test a sample in more than one gas.

In the case of bacteria, spectra were acquired in the argon environment at a delay time of 2 μs after the ablation pulse with an ICCD gate width of 20 μs duration. In helium, the delay time was set to 1 μs in order to obtain a better signal-to-noise ratio. In the case of the brass alloys, LIBS spectra were acquired in both gas environments at a delay time of 1 μs after the ablation pulse with an ICCD gate width of 20 μs duration. All delay times were determined experimentally to yield optimal signal-to-noise for the specific target and bath gas, while minimizing the broadband background emission. Specifically, the

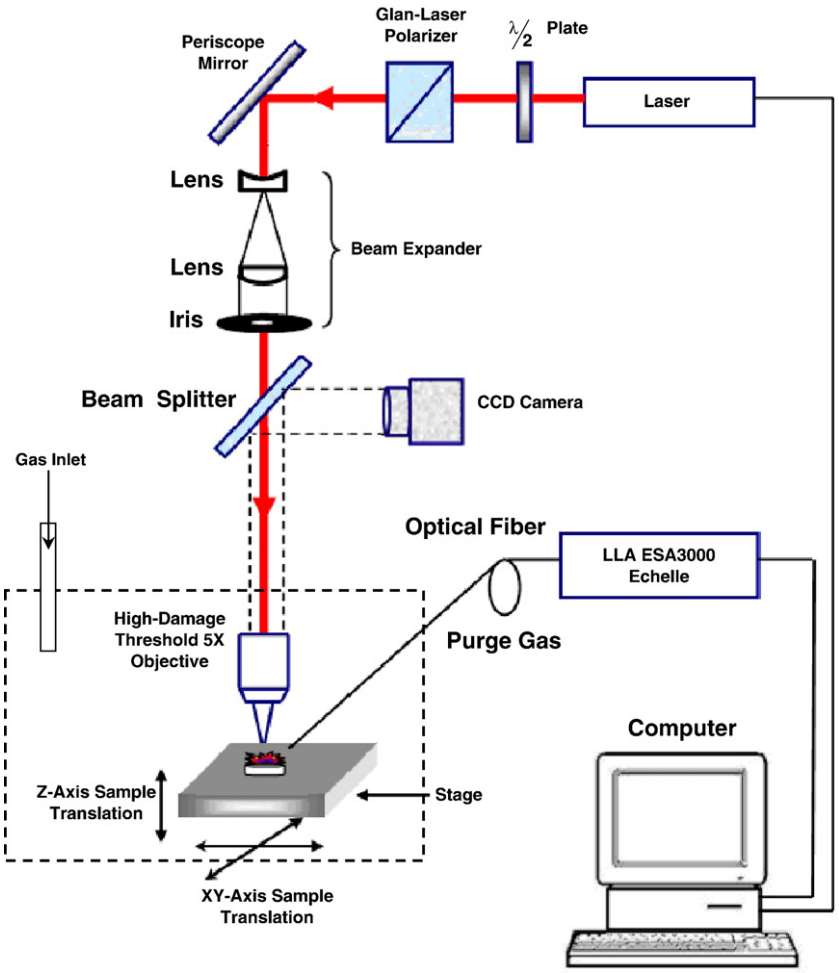

Fig. 1. A schematic diagram of the experimental setup used for the LIBS measurements of both bacteria and brass samples.

bacterial experimental conditions are the same as those used in all of our previous studies [9–12].

For the bacteria samples, five spectra were averaged at one location and five different locations were analyzed per data point, resulting in a spectrum of 25 averaged laser shots. For the brass samples, five spectra from four different locations were analyzed per data point. Each data point took approximately 20–30 s to acquire, mostly limited by ICCD readout speed. Sequential dual-gas testing was performed by preparing the samples as described below, then acquiring the desired number of spectra sequentially in a single buffer gas. The purge gas box was then flushed with the new gas (which took about 1 min), and an equal number of spectra were acquired in the new gas. In this way the purge box only needed to be flushed once per sample. The argon and helium data were analyzed together only later in software, so the order of gas testing was not important. For discrimination of an unknown sample, when repeated measurements would not typically be made, one spectrum would be acquired in one gas (30 s) the chamber would be flushed (1 min), and the second spectrum acquired in the second gas (30 s). This process does slow data acquisition, but only by a factor of two, and could be improved by reducing the size of the purge chamber which would decrease the time to displace the old buffer gas with the new one.

2.2. Bacteria sample preparation

Bacteria were grown overnight at 37 °C in nutrient broth. They were tested routinely for genetic purity. They were then streaked on trypticase soy agar (TSA) plates for single colony isolation. Bacteria were cultured for 12 h at 37 ° C in an incubator. Suspensions were created by harvesting the bacteria from culture and semi-liquid pellets were collected after centrifuging at 5000 rpm for 3 min at room temperature. Specimens of two highly similar bacteria, *E. coli* C and *E. coli* HF4714 (both non-pathogenic strains of *E. coli*) were analyzed. For comparison, a significantly different bacterium *Streptococcus mutans* was also analyzed [10,12].

2.3. Cu–Zn brass alloys

The brass alloy samples were chosen to provide a simple, well-behaved test system. Four-brass alloys (McMaster-Carr) were used: alloy 464 (unleaded naval brass) which contains a high zinc content, alloy 360 (free-machining brass), alloy 353 (machinable and formable engravers brass) which contains a lower lead content, and alloy 260 which represents a simple copper–zinc alloy. The compositions of these four alloys as provided by the manufacturer are given in Table 1. Samples were machined to a 2 cm × 2 cm size and the surface was prepared by cleaning with acetone to remove any organic chemical contaminants on the surface. After that, the acetone was rinsed off with methanol. No attempt was made to remove the inorganic contaminants. A single 2 cm × 2 cm sample was used for each alloy.

Table 1
The composition of the four brass alloys used in this study.

Alloy DFA #	Name	Alloy number	Composition
1	Naval brass	Alloy 464	60% Cu 0.8% Sn 39.2% Zn
2	Ultra-machinable brass	Alloy 360	60–63% Cu 2.5–3.7% Pb 35–37% Zn
3	Machinable and formable engravers brass	Alloy 353	55–60% Cu 0.5–1.5% Al 0.4% Pb 39% Zn
4	Formable cartridge brass	Alloy 260	68.5–71.5% Cu 0.07% max Pb 28.5–31.5% Zn

3. Results and discussion

3.1. Brass samples

Typical LIBS emission spectra from one of the brass samples obtained in the ambient atmospheres of argon and helium are shown in Fig. 2. The spectra are dominated by emission from Cu, Zn, Pb, C, and Al, and they also contain emission from Na and Ca. In the case of argon gas, 2(a), the intensity of the spectral lines was much higher than that for helium, 2(b). These two spectra were taken with different detector amplification settings to eliminate ICCD bloom and pixel saturation, so the vertical scale is not consistent from 2(a) to 2(b). The ICCD was set to a much higher amplification (image intensifier voltage) while acquiring spectra in helium than it was while acquiring spectra in argon due to the much stronger emission from the argon plasma. This can be explained by the fact that argon produced a higher plasma temperature and therefore the excitation of analyte atoms was more efficient than that in the case of helium. Moreover, the spatial confinement of the plasma in argon was stronger than that in helium, and this will directly affect the temperature of the produced plasma.

The strongest emission lines observed in both spectra are listed in Table 2. The intensities of 15 of these emission lines of Cu, Zn, C, Na, Al, Pb, and Ca marked with an asterisk in Table 2 were analyzed in every spectrum by nonlinear least squares fitting of a Lorentzian line shape to the emission curve. These 15 lines were chosen specifically to produce the most effective discrimination between samples. As is typical, the intensity was determined to be the background-subtracted integrated area under the curve. This area was determined by the commercial software integrated with the spectrometer data acquisition program (ESAWIN). The intensity of each line was divided by the sum of all line intensities in order to normalize for shot-to-shot fluctuations. This procedure is necessary when dealing with the spectra from the highly variable bacterial specimens, and was therefore performed on the brass data as well. After this normalization, these relative line intensities constituted 15 independent variables and were then input into a commercial program (SPSS Inc., SPSS v16.0) which performed a discriminant function analysis (DFA).

Discriminant function analysis is a data analysis technique which is similar to analysis of variance, but which is used to predict and quantify group memberships between two or more distinct groups. DFA uses a set of independent variables (the emission intensities) from each spectrum (each spectrum is treated as a single data point) to predict the group membership of that particular spectrum in three basic steps. First, a set of orthogonal discriminant functions is constructed from the data sets from all the groups. In this step, a canonical correlation analysis produces a set of canonical discriminant functions which are essentially the eigenvectors of the data expressed in a basis that maximizes the difference between groups. For a discrimination between N groups, N-1 discriminant functions (DF) are constructed with the first canonical discriminant function (denoted DF1) accounting for more of the variance between groups than the second canonical discriminant function (DF2), which accounts for more of the variance than the third canonical discriminant function (DF3), etc.

Second, a test for significance in the discriminant functions is performed. This is done by performing a check on the differences in the means of the groups. The null hypothesis (which is disproved if a real, significant difference exists between groups) assumes that all data is sampled from a single normal distribution with mean μ and variance σ^2. If the groups are significantly different, they will exhibit means that differ by an amount significantly greater than the variance.

In the last step, if significant differences between groups are observed, the group membership of each data spectrum is predicted

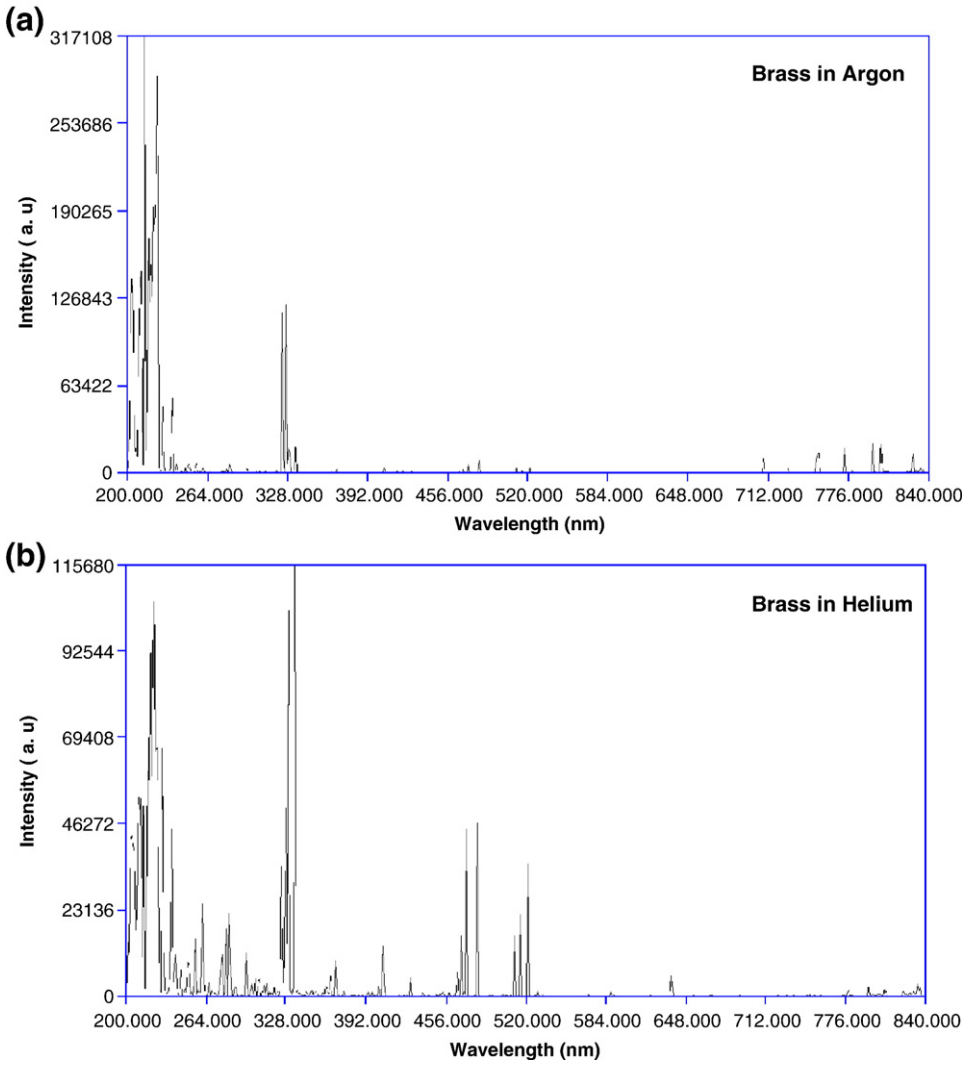

Fig. 2. LIBS emission spectra for one of the brass samples in (a) an argon environment and (b) a helium environment at atmospheric pressure.

based on the calculated canonical discriminant function scores (DF scores) for each data spectrum. The identity of each data point is calculated in a cross-validation or "leave-one-out" classification. In this test, a single data point is omitted during the construction of the discriminant functions. DF scores are calculated for the missing point using the new functions, and the unknown point is assigned a group classification on the basis of these scores. Therefore rule sets for classification are always created from "known" samples, but the specificity results are always obtained from "unknown" or unidentified samples and all data points are tested as unknown.

When used to discriminate similar spectra, such as those obtained from bacteria, typically almost all of the variance (upward of 90%) was described by only the first two canonical discriminant functions. Therefore plots are often presented showing only the first two discriminant function scores for each spectrum (such as are shown in Figs. 3–6). In these plots, discriminant function score one, representing the most distinct or obvious differences between spectra, is used as the abscissa, while discriminant function score two is used as the ordinate. Spectra from members of the same group exhibit scatter about a mean μ which is not a value, but an *N-1* dimensional vector. The within-group variance is a measure of that scatter and is significantly less than between-group variance. Any increase of the vector difference between group-centroids, or the DF scores of the centroids, is indicative of an increase in discrimination.

Fig. 3 shows a DFA plot of all brass samples tested in an argon atmosphere. Each colored object in the plot represents an entire spectrum (there are roughly 50 spectra per category). In this analysis, although three canonical discriminant functions were used to characterize the four groups, most of the discrimination was performed by the first two functions. The DFA analysis showed that 88.6% of the variance between groups was represented by discriminant function one (DF_1) and 10.5% by discriminant function two (DF_2).

Another parameter returned by the SPSS DFA is called the structure matrix, which shows the correlations of each variable with each discriminant function. Typically, identifying the largest absolute correlations between specific emission lines and each discriminant function can help determine which elements play a crucial role in the discrimination provided by that function (plotted along one axis of the plot). Shown in Table 3 is the structure matrix from the analysis of the LIBS spectra from the four brass alloys ablated in argon. The first column identifies the specific emission lines given by the element symbol and the wavelength of the transition, while the other three "function" columns show the absolute correlations between the line and that particular discriminant function. As can be seen, each predictor variable is correlated with each function, but the strongest overall correlation for each variable is indicated with an asterisk. The SPSS program then orders the predictor variables in descending order on the basis of the absolute value of their strongest correlation only,

Table 2
The strongest emission lines observed in brass LIBS plasmas acquired in argon and helium.

Wavelength (nm)	Line identification
202.547	Zn II
204.380*	Cu II
213.855*	Zn I
217.000*	Pb I
218.177*	Cu I
219.227*	Cu II
221.811	Cu II
223.007	Cu I
247.856*	C I
261.837	Cu I
282.437*	Cu I
283.305*	Pb I
324.755	Cu I
330.258	Zn I
334.502	Zn I
363.957*	Pb I
368.346*	Pb I
393.366*	Ca II
396.152*	Al I
406.265	Cu I
465.112	Cu I
468.014	Zn I
472.215*	Zn I
481.053	Zn I
510.554	Cu I
515.325	Cu I
521.820	Cu I
588.995*	Na I
589.593*	Na I

*Lines used in the DFA.

first for DF1, then DF2, etc. For example, in Table 3, the zinc line at 213 nm has a correlation of −.457 with DF1 while the Cu line at 219 nm has a correlation of only .212. But the zinc 213 nm line has it strongest correlation (−.478) with DF2, therefore it is listed lower on the list than the copper line, because function 2 accounts for less of the overall variance than does function one. This does not indicate that the 213 nm zinc line does not correlate with DF1, it indicates that it correlates most strongly with DF2. Similarly, the copper line at 204 nm has a correlation with DF1 of .133, yet it is listed last in the structure matrix, because it is most strongly correlated (−.596) with DF3, which accounts for less of the variance than DF1 or DF2. The "a" next to the Ca 393 nm line indicates it was determined that the line

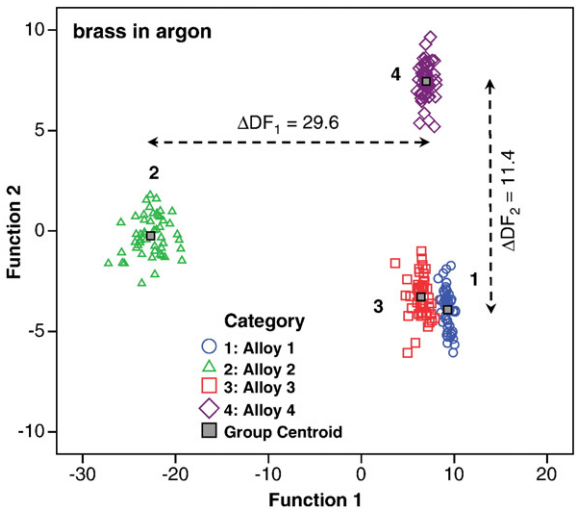

Fig. 3. A discriminant function analysis plot showing the first two discriminant function scores of LIBS spectra obtained from four brass samples in argon.

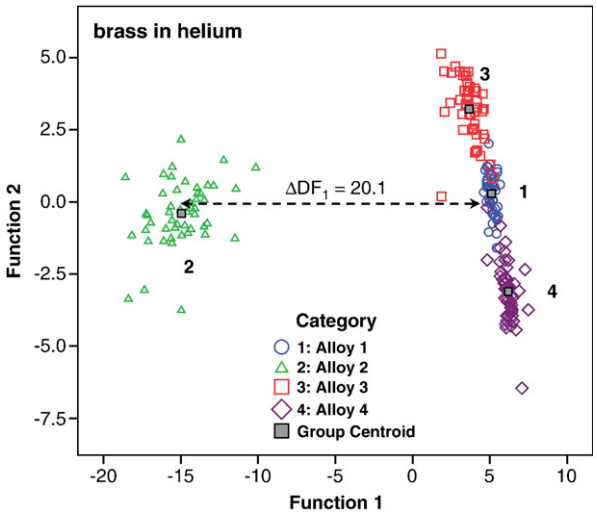

Fig. 4. A discriminant function analysis plot showing the first two discriminant function scores of LIBS spectra obtained from brass samples in helium.

not used in the analysis most likely due to statistical insignificance. Although included, the sodium lines played very little role in the discrimination, as one would expect.

From Fig. 3, it can be seen that there is an obvious difference between group two and the other three brass samples. The structure matrix of this analysis shown in Table 3 indicates it is primarily the lead content that was used to construct DF1. This result confirms the fact that alloy 2 contained more lead than the other alloys as shown in Table 1. According to this analysis, despite possessing similar spectra, the DFA of samples tested in Ar achieved an overall cross-validation (leave-one-out) classification accuracy of 99.5% (199 out of 200 correct), which indicates the benefit of using LIBS as a technique for the rapid identification of alloys and discrimination between brass samples.

In order to the study the effect of helium on our discrimination, the same samples were tested in a helium environment. Fig. 4 shows the results of the DFA performed on LIBS spectra acquired from the four brass samples. The DFA analysis showed that 91.5% of the variance between groups was represented by DF_1, 6.1% by DF_2, and 2.3% by DF_3. In the leave-one-out analysis, a classification accuracy of 97.0% (194 out of 200 correct) was achieved. In this analysis different correlations

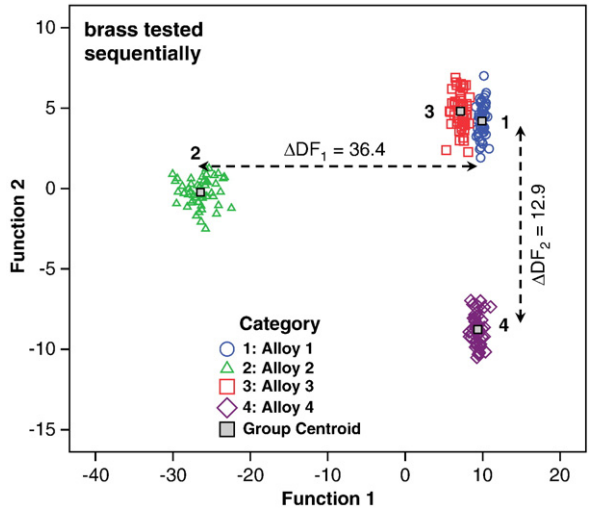

Fig. 5. A discriminant function analysis plot of brass samples tested in both gases sequentially. This data did not take substantially longer to acquire than that taken in a single gas atmosphere and discrimination is enhanced.

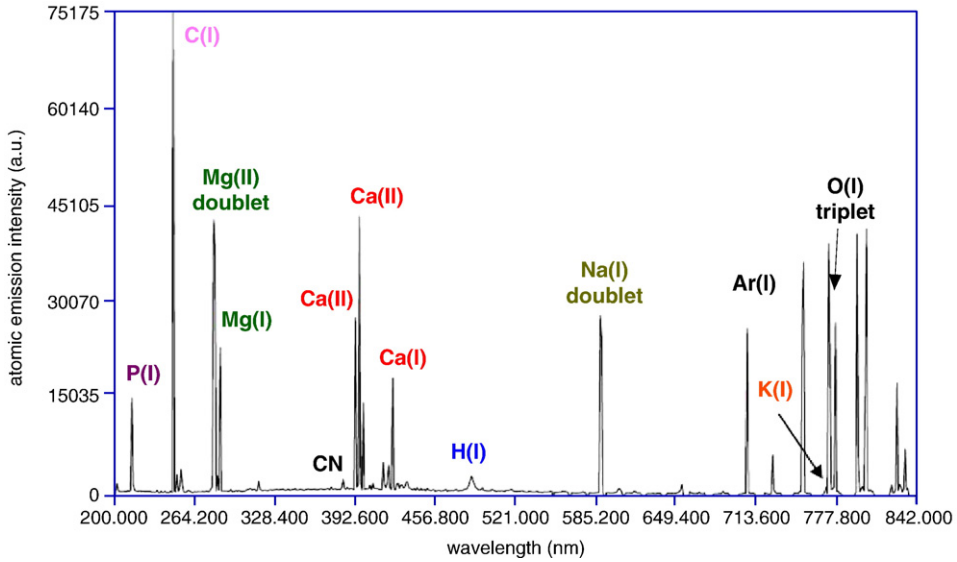

Fig. 6. A typical LIBS spectrum of *E. coli* ablated in argon. The emission lines are identified.

between spectral lines were used to construct different discriminant functions. This can be explained by the different relative emission intensities from the various elements (observed in Fig. 2) due to different plasma temperatures compared to what was observed in the argon environment. The structure matrix of the four samples tested in the helium environment, Table 4, shows this difference.

When the two 15-line spectral fingerprints obtained from the samples tested in both argon and helium were combined to form a single 30-spectral line fingerprint for the alloy, an overall 100% classification accuracy was achieved. DFA plots of the four alloys as shown in Fig. 5 showed that the distances between the group centroids (center of mass for the distribution of measurements) were increased. This is indicative of an enhancement in the ability to distinguish one alloy from another. For example, the distance between the centroids of alloy one and alloy two was increased by almost 100% over what was observed in helium and by 15% over what was observed in argon. Although alloys 1 and 3 appear unchanged, the distance between the centroids of alloy 1 and alloy 3 increased by over 65% in function 3 (not shown in Figs. 3 or 5) over what was observed in argon. Although DF3 is typically not plotted, it does indeed contribute to discrimination and classification. Also, the scatter of measured data points around the centroids was reduced. This result showed the benefit of using dual ambient gases in sequence for an enhancement of discrimination between the samples. Because our sample chamber was small, these gases could be quickly cycled in and out in about a minute, adding very little complexity to the analysis for a modest increase in discrimination ability.

An increase in the discrimination of brass (as evidenced by the slight increase in classification accuracy and the increase in the separation of group means) was seen, but was not large due to the ease with which the samples could be discriminated in argon alone due to the differences in the samples.

3.2. Bacteria results

Our previous results using a DFA to identify/discriminate LIBS spectra obtained from bacterial samples showed that bacteria can be efficiently discriminated when tested in air or in argon or helium [9–12]. However, the highly similar nature of the spectra from different strains of a single species could eventually limit the ability to identify samples in a mixed, contaminated, or low concentration sample. Based on the previous study with the Cu–Zn brass alloys, a similar study was performed to demonstrate an enhanced discrimination between two strains of *Escherichia coli* (a Gram-negative bacterium) and a Gram-positive bacterium when LIBS spectra were sequentially obtained in two

Table 3
The structure matrix for the DFA of four brass alloys ablated in an argon atmosphere.

	Function		
	1	2	3
C247.856	−.620*	−.054	−.015
Pb283.305	−.423*	−.089	.029
Pb368.347	−.418*	−.074	−.068
Pb363.957	−.408*	−.062	−.124
Pb217.000	−.362*	−.106	.157
Ca393.366[a]	−.320*	−.041	−.191
Al396.152	−.319*	−.020	−.234
Na588.995	−.270*	−.028	−.150
Na589.593	−.240*	−.027	−.133
Cu219.227	.212	.528*	.115
Zn213.855	.457	−.478*	.193
Zn472.215	.060	−.356*	−.100
Cu218.177	.182	.293*	.161
Cu282.437	.070	.213*	−.048
Cu204.380	.133	.124	−.596*

* Indicates with which function each variable had the strongest overall correlation.
[a] Indicates that the line was not used in the analysis.

Table 4
The structure matrix for the DFA of four brass alloys ablated in a helium atmosphere.

	Function		
	1	2	3
Pb283.305	−.707*	.170	.383
Ca393.366[a]	−.686*	−.235	−.031
Pb368.347	−.680*	.035	.250
Pb363.957	−.663*	−.023	.187
Al396.152	−.608*	−.233	−.055
Na588.995	−.540*	−.183	−.085
Pb217.000	−.527*	.130	.318
Na589.593	−.463*	−.162	−.053
Cu204.380	.136*	−.047	.136
Cu282.437	.137	−.250*	.171
Cu218.177	.126	−.192*	.109
C247.856	−.296	−.034	.330*
Zn472.215	.068	.179	−.321*
Cu219.227	.150	−.079	.185*
Zn213.855	.067	.031	−.117*

* Indicates with which function each variable had the strongest overall correlation.
[a] Indicates that the line was not used in the analysis.

different gas environments. The intensities of 13 emission lines from Mg, Ca, P, Na, and C were used in the discriminant function analysis.

Typical bacterial LIBS spectra are dominated by emission from inorganic elements. A representative spectrum obtained in argon is shown in Fig. 6. Fig. 7(a) shows the results of the DFA performed on LIBS spectra acquired from *E. coli* HF4714 and Nino C and *Streptococcus mutans* in an argon environment. It is obvious from the plot that the bacterial strains are reproducibly different from each other. The analysis showed that 82% of the variance in this test was in DF_1 and 18% of the variance was contained in DF_2. The structure matrix showed that carbon and magnesium were mainly used in DF_1 to discriminate bacteria from each other while phosphorus and calcium were responsible for the discrimination in DF_2. In this analysis 96.7% (87 out of 90) of all samples were correctly classified.

The same samples were then ablated in a helium atmosphere. Fig. 7(b) shows a DFA plot for the *E. coli* and *S. mutans* specimens. In this analysis, 61% of the variance between groups was represented by DF_1 and 39% by DF_2. Of the original grouped cases, 97.8% of all data sets (88 out of 90) were correctly classified. In addition to that, the structure matrix showed sodium and magnesium were responsible for the discrimination in DF_1 while calcium and phosphorus concentrations played a stronger role in the discrimination in DF_2.

When the data from the samples tested sequentially in both gases were combined to create a 26-emission line spectral fingerprint, a 100% classification accuracy (90 out of 90) was achieved. The results of this DFA are shown in Fig. 8. Compared to testing in either gas singly, the distances between the group centroids in the DFA were increased, and compared to the brass samples, the dual-gas testing procedure had a much more pronounced effect on the separation of the group centroids. For example, the distance in DF1 between the centroids of group one (*E. coli* C) and group three (*Strep. mutans*) was increased by 70% over what was observed in helium and by 56% over what was observed in argon. The distance in DF2 between the centroids of group two and groups one and three increased by 89% over what was observed in argon and 26% over what was observed in helium. As was observed in the brass samples, the scatter of measured data points around the centroids was also reduced.

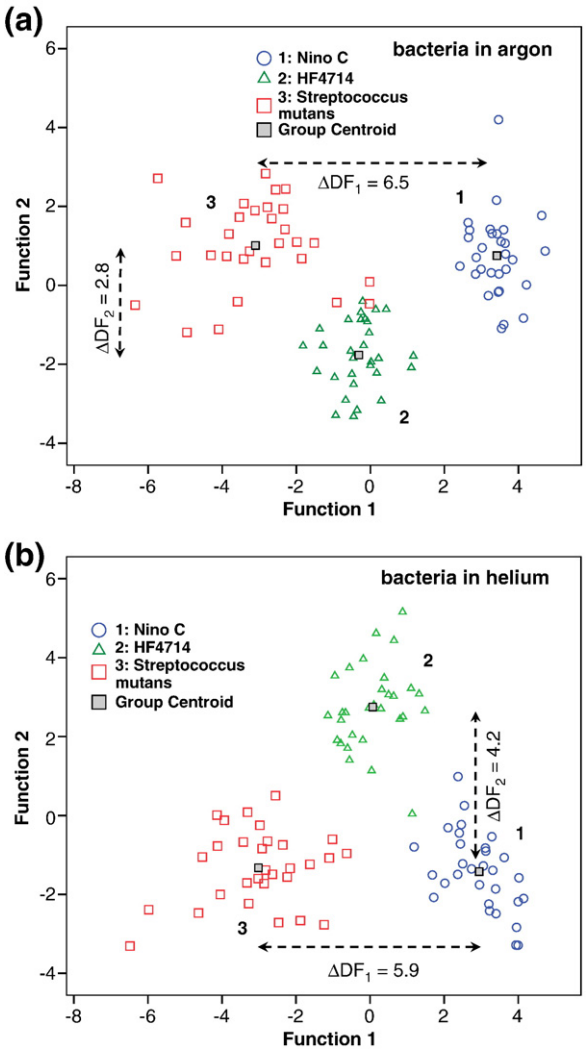

Fig. 7. (a) A discriminant function analysis plot of LIBS spectra from bacterial specimens of two strains of *E. coli* (Nino C and HF4714) and *Streptococcus mutans* ablated in an argon environment. (b) A DFA of the same three specimens ablated in a helium environment.

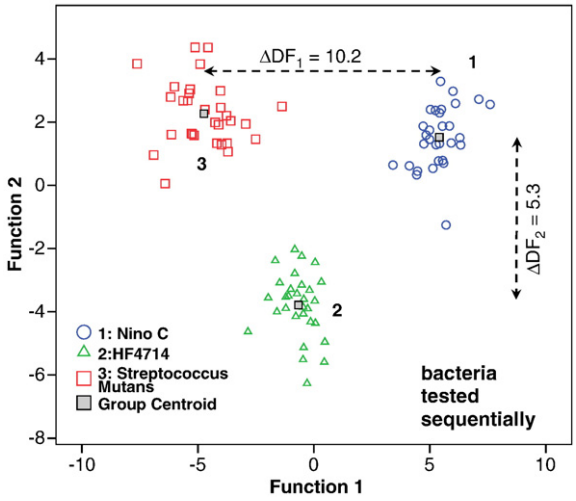

Fig. 8. A discriminant function analysis plot of three bacterial samples tested sequentially in both argon and helium. Enhanced discrimination relative to testing in either gas individually is observed.

This result demonstrates that the use of sequential dual-gas testing is most appropriate when the specimens are highly similar and difficult to discriminate. In such situations, even small gains in discrimination and classification accuracy may be advantageous. The improvement in classification accuracy involved only a small number of spectra that had previously been incorrectly classified, so future tests are called for where a lower classification accuracy (50% or less) is observed when a single gas is used. Currently, all of our bacterial specimens classify with well over 90% accuracy, typically, so the use of sequential dual-gas testing is not called for.

4. Conclusions

The emission characteristics of laser-induced plasmas are strongly influenced by the gaseous environment in which the plasma is created. Noble gases such as argon or helium are often used to improve emission and reproducibility in such plasmas. LIBS spectra from four alloys of brass and three different bacterial specimens were obtained from samples ablated sequentially in argon and then in helium. A small purge box allowed these measurement to be taken in almost the same amount of time that testing in one gas only would require. The highest spectral line intensities were obtained in argon which can be related to the higher plasma temperature.

When emission intensities from spectra acquired sequentially in argon and helium were combined to form new spectral fingerprints, an enhanced DFA discrimination was observed as evidenced by an increase in the distances between the group centroids of all the samples (in both the brass and the bacterial systems) and a reduction of the observed scatter of measured data points around the group centroids. Most importantly, the absolute accuracy of the identification/discrimination was increased from 99% to 100% in the brass

system and 97% to 100% in the bacterial system. As expected, the absolute increase in classification accuracy was smaller for the brass samples, because of the relative ease with which they could be discriminated by either gas alone. The increase in the classification accuracy of the bacterial specimens however was significant, particularly the increase in the separation between group means that was an obvious result.

This result could be useful for future identification or discrimination between several species or strains of bacteria that are highly similar to each other. In systems where large differences exist between samples and discrimination based on the observed LIBS spectrum is relatively easy, this dual-gas technique possesses little advantage over a LIBS analysis in pure argon alone.

Acknowledgements

The authors gratefully acknowledge the assistance of Dr. Sunil Palchaudhuri of the Wayne State University Department of Immunology and Microbiology for providing the bacterial specimens and for helpful discussion.

References

[1] C. Pasquini, J. Cortez, L. Silva, F. Gonzaga, Laser-induced breakdown spectroscopy, J. Braz. Chem. Soc. 18 (2007) 463–512.
[2] D. Cremers, L. Radziemski, Handbook of Laser-Induced Breakdown Spectroscopy, John Wiley & Sons Ltd., Chichester, 2006.
[3] J. Singh, S. Thakur, Laser-Induced Breakdown Spectroscopy, Elsevier, Amsterdam, 2007.
[4] V. Detalle, M. Sabsabi, L. St-Onge, A. Hamel, R. Héon, Influence of Er:YAG and Nd:YAG wavelength on laser-induced breakdown spectroscopy measurements under air or helium atmosphere, Appl. Opt. 42 (2003) 5971–5977.
[5] W. Sdorra, K. Niemax, Basic investigations for laser microanalysis: III. Application of different buffer gases for laser-produced sample plumes, Mikrochim. Acta 107 (1992) 319–327.
[6] M. Kuzuya, H. Matsumoto, H. Takechi, O. Mikami, Effect of laser energy and atmosphere on the emission characteristics of laser-induced plasmas, Appl. Spectrosc. 47 (1993) 1659–1664.
[7] R. Wisburn, I. Schechter, R. Niessner, H. Schroder, K. Kompa, Detector for trace elemental analysis of solid environmental samples by laser plasma spectroscopy, Anal. Chem. 66 (1994) 2964–2975.
[8] 0HM. Adamson, A. Padmanabhan, G.J. Godfrey, S.J. Rehse, Broadband laser-induced breakdown spectroscopy at a water/gas interface: a study of bath gas-dependent molecular species, Spectrochim. Acta Part B 62 (2007) 1348–1360.
[9] J. Diedrich, S.J. Rehse, S. Palchaudhuri, *Escherichia coli* identification and strain discrimination using nanosecond laser-induced breakdown spectroscopy, Appl. Phys. Lett. 90 (2007) 163901–1–3.
[10] J. Diedrich, S.J. Rehse, S. Palchaudhuri, Pathogenic *Escherichia coli* strain discrimination using laser-induced breakdown spectroscopy, J. Appl. Phys. 102 (2007) 014702–1–7.
[11] S.J. Rehse, J. Diedrich, S. Palchaudhuri, Identification and discrimination of *Pseudomonas aeruginosa* bacteria grown in blood and bile by laser-induced breakdown spectroscopy, Spectrochim. Acta Part B 62 (2007) 1169–1176.
[12] S.J. Rehse, N. Jeyasingham, J. Diedrich, S. Palchaudhuri, A membrane basis for bacterial identification and discrimination using laser-induced breakdown spectroscopy, J. Appl. Phys. 105 (2009) 102034–1–13.